Available online at www.sciencedirect.com

ScienceDirect

journal homepage: www.elsevier.com/locate/he

Comparison between WGS membrane reactors operating with and without sweep gas: Limiting conditions for co-current flow

María Esperanza Adrover, Daniel Borio, Marisa Pedernera *

CONICET/Planta Pilota de Ingeniería Química (PLAPIQUI), Universidad Nacional del Sur, Camino La Carrindanga km. 7, 8000, Bahía Blanca, Argentina

ARTICLE INFO

Article history:
Received 31 August 2016
Received in revised form
7 November 2016
Accepted 10 November 2016
Available online 16 December 2016

Keywords:
Reactor analysis
Membrane reactor
WGS
Limiting conversion
Sweep gas

ABSTRACT

In this work, a comparative study is carried out to analyze the behavior of a water gas shift membrane reactor operating with and without sweep gas. The present study includes thermal effects that play a key role in reaction and permeation rates involved in the membrane reactor. Based on a 1-D mathematical model, the effect of the most important operating variables on the membrane reactor performance is comparatively studied. Additionally, novel algebraic expressions are developed when operating without sweep gas, that only depend on inlet variables to calculate the limiting membrane reactor conversions and recovery values. An algebraic equation is developed to estimate limiting recovery when operating with sweep gas. The dependence of limiting membrane reactor conversion and recovery values operating with and without sweep gas on operating parameters is included. From the comparative analysis, some guidelines for an improved operation of the membrane reactor are proposed.

Introduction

A general interest has emerged recently about hydrogen as an energy vector. There are many alternatives to produce hydrogen or syngas from hydrocarbons or oxygenated compounds such as alcohols [1]. Hydrogen produced for fuel cell applications should be purified in order to avoid carbon monoxide poisoning of the PEM fuel-cell anode catalyst. To this end, the water gas shift reaction (WGSR) is extensively used not only to reduce CO contents, but also to increase hydrogen production. Since this reaction is moderately exothermic and controlled by thermodynamic equilibrium, the WGS reactor is the largest of the generation-purification system [2]. This presents a particular challenge for new WGS reactor designs. Membrane reactors constitute a promising alternative for process intensification, since hydrogen can be selectively removed from the reaction mixture and, consequently, higher conversion levels can be achieved. A review of recent advances in catalysts, palladium alloys and high temperature WGS membrane reactors can be found in the literature [3].

In order to properly design a WGS membrane reactor for hydrogen purification, it is convenient to use a mathematical model of the reactor. There are several theoretical studies about water gas shift membrane reactors [4–13]. Some authors have focussed on non-isothermal reactor operations. Chiappetta et al. [14] studied the behavior of a membrane reactor by means of a non-isothermal two-dimensional (2D) mathematical model. The authors present a sensitivity analysis of different operating variables (sweep gas flowrate, pressure and temperature). Chein et al. [15] also considered 2-D non-isothermal governing equations for the gas flow, energy transport and

* *Corresponding author.*
E-mail address: mpedernera@plapiqui.edu.ar (M. Pedernera).
http://dx.doi.org/10.1016/j.ijhydene.2016.11.075

species transport in order to describe the influence of H_2O/CO molar ratio, pressure and sweep gas flowrate on the conversion and hydrogen recovery of a WGS-membrane reactor. Sanz et al. [16] used a 2D model, considering the mass, energy and momentum balances, to simulate a water–gas-shift membrane reactor. The momentum balance was adapted to simulate the non-ideal flow pattern of the membrane reactor. The results were validated with lab-scale experimental data. Brunetti et al. [17] analyzed the effect of increasing operating pressure in a WGS membrane reactor operating without sweep gas, by means of a non-isothermal unidimensional mathematical model. Koc et al. [18] developed a non-isothermal mathematical model under steady-state and dynamic conditions in order to study the behavior of a membrane reactor from a safety point of view. Marín et al. [19] studied the influence of the main operating parameters (inlet temperature, pressure, space velocity, etc.) using a 2D reactor model that takes into account radial and axial variations of properties (including bed porosity), setting mass, energy and momentum differential balances. They concluded that space velocity and pressure are the most important parameters affecting reactor performance for membrane reactors. Using a 3D numerical model, Chein et al. [20] explored the effect of the design of the permeation side on the performance of membrane reactors. The authors studied flow pattern, flow rate, temperature and sweep-gas flow type effects on the WGS membrane reactor performance. Hla et al. [21] developed a CFD (2D, non-isothermal) model of a high temperature WGS catalytic membrane reactor in order to maximize the reactor performance by finding the optimum range of operating parameters. The validity of the model was checked using experimental data.

On the other hand, there are a lower number of studies focusing on higher-scale reactors, in which thermal effects are particularly relevant. Koukou et al. [22] presented a mathematical model that considers mass-dispersion effects to simulate an adiabatic membrane reactor at industrial scale. Markatos et al. [23] extended the mathematical model including the heat dispersion effects. The influence of the operating pressure and thermal gradients on the reactor performance was addressed in a previous theoretical contribution [24] that considered a multi-tubular membrane reactor with the catalyst in the shell and co-current flow of the permeated hydrogen inside the tubes. However, no sweep gas was considered to obtain pure hydrogen and eliminate the need of a downstream purification unit. A comparative study of the effect of different sweep gases on a membrane reactor was carried out only for methane steam reforming reaction [25]. The authors found that the temperature profiles on the reaction and permeation sides using steam as sweep gas were almost the same as using nitrogen. To our knowledge, no comparative studies between a WGS membrane reactor operating with and without sweep gas have been carried out.

In order to carry out this comparative study, it is useful to know the *limiting* CO conversion and *limiting* H_2 recovery values of a membrane reactor operating with and without sweep gas. For each operating condition, the *limiting conversion* is the maximum conversion that would be reached in the membrane reactor if the amount of catalyst and the available membrane area were infinite. Some studies have estimated the limiting conversion of a membrane reactor. Barbieri et al. [26] calculated the equilibrium of a membrane reactor where methane steam reforming was carried out using steam as sweep gas. To this end, an iterative procedure was proposed in which all reactions achieved the equilibrium and afterwards permeation occurred under isothermal conditions. Additionally, simulation results of non-isothermal and adiabatic reactor long enough to achieve equilibrium behavior were included. Marigliano et al. [27] extended the study of Barbieri et al. [26] to a WGS Pd-based membrane reactor. The authors employed the same iterative tool to estimate equilibrium conversion and concluded that equilibrium conversion diminishes with temperature and increases with sweep gas flowrate and reference component flowrate ratio. The authors also found that equilibrium conversion increases with pressure. Hara et al. [28] developed an approach to estimate the limiting conversion of an isothermal membrane reactor without integrating differential equations. Methane steam reforming was adopted as model reaction and steam acting as sweep flows under countercurrent configuration. Gallucci et al. [29] introduced non-linear algebraic expressions to estimate equilibrium conversion of a membrane reactor where methane steam reforming and WGS reaction take place when operating with sweep gas.

In the present work, the tools proposed by Gallucci et al. [29] for the limiting conversion are extended to calculate the limiting membrane reactor recovery values when operating with sweep gas. For the case of sweep gas absence, to our knowledge, there are no algebraic expressions to estimate the limiting conversion and limiting recovery under co-current flow. This work presents these algebraic tools which, in combination with the simulation model, are employed to compare the performance of two co-current multi-tubular membrane reactors operating with and without sweep gas, with special interest in thermal effects. A co-current flow was selected because it has been demonstrated that under certain operating conditions the countercurrent operation shows multiplicity of steady-state [30].

The most critical operating variables (sweep gas flowrate, inlet temperature and pressure) are analyzed, aiming to obtain some guidelines for an improved operation of the membrane reactor.

Mathematical model

The design for the MR is shown in Fig. 1. The catalyst is packed in the shell side (retentate side) and many membranes tubes are considered in this study. Two membrane reactor designs are studied comparatively. **Design 1** (D1) implies operating without sweep gas in the permeate side, i.e., the driving force is achieved by means of pressure increments in the retentate side and the permeate side is pure hydrogen. When **Design 2 (**D2) is considered, pressures at both sides of the membrane are equal and the driving force depends on the sweep gas flowrate fed on the permeate side (Fig. 1). Conversely to D1, in D2 the permeated hydrogen should be purified downstream the membrane reactor.

In order to describe the behavior of a membrane reactor operating under steady state operation, a 1-D pseudohomogenous model is considered under the following hypothesis:

(a) Axial dispersion terms of mass and energy are neglected; (b) Composition and thermal gradients in the radial

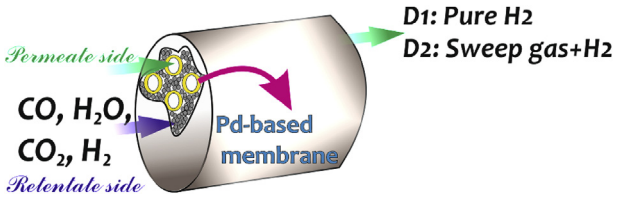

Fig. 1 – Membrane reactor scheme.

coordinate are neglected; (c) Isobaric conditions; (d) Ideal membrane only permeable to hydrogen (infinity selectivity); (e) co-current configuration is assumed [30]; (f) the palladium layer is the mass-transfer controlling resistance [31]. (g) Concentration polarization phenomena is neglected [32,33]. This hypothesis is not valid for membrane thickness lower than that used in the present article [33,34]; (h) the enthalpy associated with permeating hydrogen is neglected [35]. The contribution of this term was evaluated in detail and was found as negligible within a wide range of operating conditions [36].

The Langmuir–Hinshelwood kinetic model proposed by Podolski and Kim [37] is selected to evaluate the reaction rate (Eq. (6)) and the Fe–Cr catalyst considered in the present study usually operates between 310 and 450 °C [38].

Under the stated hypothesis, the reaction model is: The convective heat transfer coefficient in the retentate side (α_r) is estimated following the guidelines proposed by Dixon [40]. In order to estimate α_r, the wall heat transfer coefficient (α_w) and the effective radial heat conductivity in the packed-bed (λ_{er}) are calculated using the correlations proposed by Dixon and Cresswell [41].

These correlations have been developed for a tubular configuration. However, they could be used for annular configuration as proposed by De Falco et al. [42] by means of an equivalent radius (r_{eq}). The heat transfer coefficient corresponding to the permeate side (α_P) is evaluated for laminar, fully developed flow from Incropera and DeWitt [43]. The heat conductivities of the support ($\lambda_{Al_2O_3}$) and the Pd membrane (λ_{Pd}) are obtained from Hussain et al. [44] and Incropera and DeWitt [43], respectively.

The mathematical model is valid for both membrane reactor designs, i.e., D1 and D2. However, the boundary conditions depend on the membrane reactor design (Eq. (10)). The composition and temperature axial profiles on both sides of the membrane, were obtained by integrating the set of differential and algebraic Eqs. (1)–(9) by means of a Gear algorithm. The mathematical model has been validated by experimental results obtained by Criscuoli et al. [4] under isothermal conditions and has been extensively discussed by the authors [24,45].

The design parameters, permeation model parameters and the operating conditions used in the simulations are presented in Table 1. Kinetic model parameters are presented in Table 2. It is important to remark that the maximum admissible operating temperature should be $T_{MAX} = 500$ °C in order to avoid WGS catalyst deactivation due to sintering [46]. On the other hand, the membrane reactor should not operate at

Shell side (catalyst bed)

Mass balances

$$\frac{dF_{CO}}{dz} = A_T r_{CO} \rho_B \quad (1)$$

$$\frac{dF_{H_2}}{dz} = A_T(-r_{CO})\rho_B - \pi n_t d_{te} J_{H_2} \quad (2)$$

Energy balance

$$\frac{dT}{dz} = \frac{A_T \rho_B (-r_{CO})(-\Delta H_r) - \pi n_t d_{ti} U (T - T_P)}{\sum_{i=1}^{N} F_j C_{pj}} \quad (3)$$

Kinetic model:

$$r_{CO} = \frac{k}{60} K_{CO} K_{H_2O} \frac{\left(p_{CO} p_{H_2O} - \frac{p_{CO_2} p_{H_2}}{Keq}\right)}{\left(1 + K_{CO} p_{CO} + K_{H_2O} p_{H_2O} + K_{CO_2} p_{CO_2}\right)^2} \quad (6)$$

Kinetic (k) and adsorption equilibrium constants (K):

$$K_i = \exp\left(-\frac{\Delta H_i}{RT} + \frac{\Delta S_i}{R}\right) \quad i = CO,\ H_2O,\ CO_2 \quad (8)$$

Boundary conditions:

$$\text{At } z = 0: \quad F_j = F_{jo} \ \text{ for } j = 1,\ 2\ldots.,N \qquad T = T_o; T_P = \begin{cases} T_o (D1) \\ T_{Po} (D2) \end{cases}; \qquad F_{H_2,P} = 0; F_{SG} = \begin{cases} 0\ (D1) \\ \neq 0\ (D2) \end{cases} \quad (10)$$

Tube side (permeate)

Mass balances

$$\frac{dF_{H_2,P}}{dz} = \pi d_{te} J_{H_2} \quad (4)$$

Energy balance

$$\frac{dT_P}{dz} = \frac{\pi d_{te} n_t (T - T_P)}{\left(F_{H_2,P} C_{pH_2} + F_{SG} C_{pSG}\right)} \left[U \frac{d_{ti}}{d_{te}}\right] \quad (5)$$

Sievert's law [39]:

$$J_{H_2} = \frac{Q_0 e^{\left(-E_p/RT\right)}}{\delta} \left[\sqrt{p_{H_2}} - \sqrt{p_{H_2,P}}\right] \quad (7)$$

Overall heat transfer coefficient (U):

$$U = \frac{1}{\frac{d_{ti}}{d_{tm}} \frac{1}{\alpha_r} + r_i \frac{\ln(d_{te}/d_{ti})}{\lambda_{Al_2O_3}} + r_i \frac{\ln(d_{tm}/d_{te})}{\lambda_{Pd}} + \frac{1}{\alpha_P}} \quad (9)$$

Table 1 – Design parameters, permeation model parameters and operating variables.

Parameter	Value
Design parameters	
Tube length, L	0.29 m
Internal tube diameter, d_{ti}	0.008 m[a]
External tube diameter, d_{te}	0.0134 m[a]
Internal shell diameter, d_c	0.145 m
Number of tubes, n_t	63[b]
Palladium thickness	60 μm
Permeation parameters	
Preexponential factor, Q_0	$7.7 \cdot 10^{-5}$ mol/(s m atm$^{0.5}$)[c]
Activation energy of hydrogen permeability, E_p	16,300 J/mol[c]
Inlet conditions	
Total flowrate, F_{To}	7.7 Nm^3/h
Permeate pressure, P_P	1 atm
Inlet composition	
CO, %	7.97[d]
CO_2, %	10.99[d]
H_2, %	43.48[d]
H_2O, %	31.88[d]
CH_4, %	5.68[d]

[a] Criscuoli et al. [4].
[b] Adrover et al. [24].
[c] Barbieri et al. [39].
[d] Francesconi et al. [2].

Table 2 – Kinetic model parameters.

	Enthalpy factor ΔH_i, cal/mol	Entropy factor ΔS_i, cal/mol K
k, mol/(g cat)(min)	29,364	40.32
K_{CO}, atm^{-1}	−3064	−6.74
K_{CO_2}, atm^{-1}	−12,542	−18.45
K_{H_2O}, atm^{-1}	6216	12.77

temperatures lower than $T_{MIN} = 300$ °C in order to minimize the CO adsorption on the membrane [47,48]. It should be noticed that the inlet composition resembles the outlet stream of an ethanol reformer operating under equilibrium conditions at 550 °C and presents high amounts of H_2.

Results and discussion

In this work, the performance of a water gas shift membrane reactor is studied for two different membrane reactor designs. The most critical operating variables are analyzed and a comparison between both membrane reactor designs is included. Additionally, algebraic equations are proposed to estimate the limiting CO conversion and hydrogen recovery values.

Membrane reactor operating without sweep gas (D1)

The most critical operating variables when operating the membrane reactor without sweep gas (D1) are the inlet temperature (T_o) and retentate pressure (P).

Study of main operating variables

Fig. 2 shows axial profiles of CO conversion (a), temperature (b) and hydrogen recovery (c) for different inlet temperatures (T_o) that correspond to an operating pressure of 5 atm (retentate side). Hydrogen recovery (R) is the ratio of permeated hydrogen to the total amount of hydrogen, i.e., hydrogen in the retentate and permeate sides and is defined by the following Eq. (11):

$$R = \frac{F_{H_2,P}}{F_{H_2,P} + F_{H_2}} \tag{11}$$

Fig. 2a and b shows that the membrane reactor presents two different zones. At the entrance of the reactor the conversion and temperature increase rapidly and then the increase is less pronounced for different inlet temperature values because the reaction rate achieved a nearly constant value. It is important to note that the outlet conversion values are higher as T_o decreases. For the operating conditions under study, the inlet temperature that maximizes the CO conversion is 320 °C.

It is worth mentioning that CO conversion presents with temperature the typical behavior of a conventional reactor operating under equilibrium conditions, i.e., low temperatures lead to low conversion values due to kinetic reasons and as temperature increases, the conversion reaches a maximum value and then starts to decrease with T_o. These results are not presented because lower feed temperature values are not of practical interest.

Conversely to the dependence of CO conversion with respect to T_o, hydrogen recovery increases as the feed

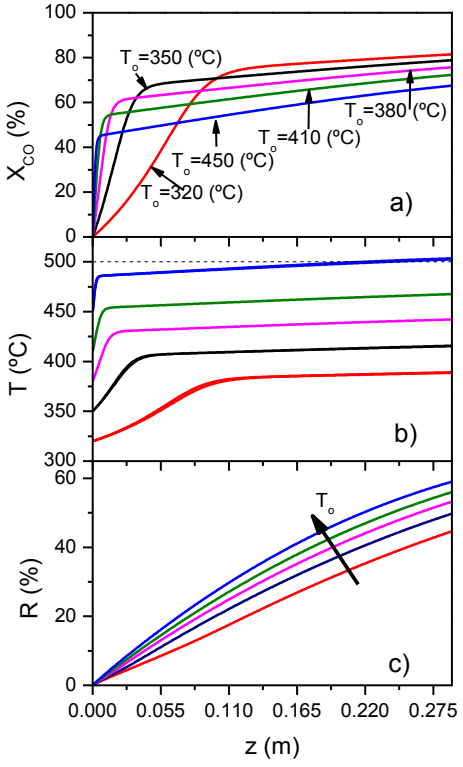

Fig. 2 – CO conversion (a), temperature (b) and hydrogen recovery (c) axial profiles at different T_o, corresponding to D1. P = 5 atm.

temperature increases (Fig. 2c), because permeation is a temperature activated process. As a consequence, the feed temperature that maximizes CO conversion (T_o = 320 °C) is different from that which maximizes hydrogen recovery (T_o = 450 °C). It is important to note that if the main goal of the membrane reactor is to convert CO, lower operating temperatures are optimal. However, if the aim of the membrane reactor is to produce pure H_2 that would be fed into a PEM fuel cell, higher operating temperatures are advisable. In the multitubular membrane reactor under study, only a small fraction of the total hydrogen (approximately 10%) is generated inside the water gas shift reactor, mostly comes from the upstream reformer. This fact explains the different behaviors observed in Fig. 2a and b where at the entrance of the reactor domain the reaction rate and afterwards, the permeation rate domains the reactor behavior.

In order to clarify the results showed in Fig. 2, Fig. 3 presents the axial profiles of the equilibrium constant (K) (Fig. 3a) and hydrogen partial pressures (p_{H2}, $p_{H2,P}$) at both sides of the membrane (Fig. 3b), respectively, for two of the operating conditions showed in Fig. 2 (T_o = 320 °C y T_o = 450 °C). Fig. 3a shows the typical behavior of a fixed bed reactor operating under equilibrium conditions, i.e., as temperature increases, the equilibrium constant diminishes, as expected for exothermic reactions. In Fig. 3b hydrogen partial pressure on the retentate side presents lower values as the inlet temperature increases, for almost the whole reactor length due to lower conversion levels achieved in the membrane reactor (see Fig. 3a) and due to permeation process that is activated with temperature. To sum up, as feed temperature increases, K and hydrogen partial pressure decreases. However, the effect of the reduction in K prevails over the effect of the partial pressure reduction, leading to lower reaction rates and consequently, a lower CO conversion.

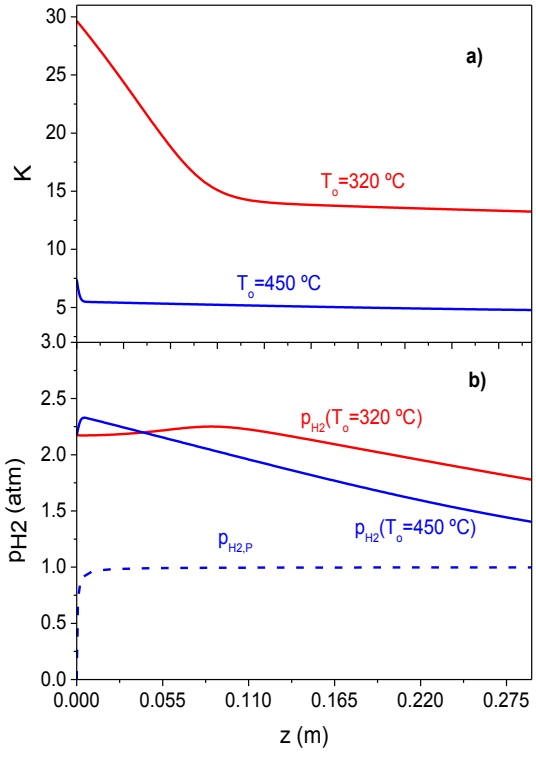

Fig. 3 – K (a) and p_{H_2} (b) axial profiles at both sides of the membrane for T_o = 320 °C and T_o = 450 °C.

Estimation of the limiting condition

In order to determinate the operating variables that could optimize the membrane reactor operation, it is mandatory to establish the limiting values for the CO conversion and H_2 recovery of the membrane reactor.

The limiting conversion of a membrane reactor could be estimated under the following hypothesis:

- Chemical equilibrium (r_{CO} = 0),
- No driving force for mass transfer, i.e., hydrogen partial pressures at both sides of the membrane are equal: $p_{H_2} = p_{H_{2,P}}$ (co-current configuration).

At equilibrium conditions, the composition of the ideal mixture could be described from the water gas shift equilibrium constant:

$$K = \frac{y_{CO_2} y_{H_2}}{y_{CO} y_{H_2O}} = \frac{F_{CO_2} F_{H_2}}{F_{CO} F_{H_2O}} \tag{12}$$

From the stoichiometric balances for the species involve in the reaction and taking into account that, at equilibrium conditions, the hydrogen partial pressures at both sides of the membrane are equal, Eq. (13) is obtained:

$$f\left(X_L^{MR}\right) = exp^{(K)} - \frac{\left(F_{CO_2,o} + F_{CO,o} X_L^{MR}\right)\left(F_{T,o} - \frac{F_{H_2,o} + F_{CO,o} X_L^{MR} - \frac{P_P F_{To}}{P}}{1 - \frac{P_P}{P}}\right)}{F_{CO,o}\left(1 - X_L^{MR}\right)\left(F_{H_2O,o} - F_{CO,o} X_L^{MR}\right)} \frac{P_P}{P} = 0 \tag{13}$$

The aforementioned equation allows to estimate the limiting conversion of a co-current membrane reactor operating without sweep gas under atmospheric pressure on the permeate side. It should be noted that the limiting conversion of a membrane reactor, X_L^{MR}, depends on molar flowrates, feed temperature and operating pressure. It is worth mentioning that Eq. (13) applies only to co-current configuration because hydrogen partial pressure in the retentate side decreases along the reactor, while hydrogen partial pressure in the permeate side remains equal to 1 atm. As a consequence, both hydrogen partial pressures could be equal and satisfy permeation equilibrium.

Fig. 4 presents results corresponding to X_L^{MR}, obtained from Eq. (13) for different operating pressure and temperature values. The equilibrium curve X_{eq}^{CR}, corresponding to a fixed bed reactor without hydrogen permeation is included. It is possible to observe that the limiting conversion of a membrane reactor strongly depends on operating pressure while equilibrium conversion of a fixed bed reactor does not. Additionally, this dependence is lower as pressure increases. In the MR, pressure benefits the limiting conversion while temperature does not, i.e., the curves decay with temperature. However, this disadvantageous effect on the limiting conversion is attenuated at higher pressures because permeation is so effective that the water gas shift reverse reaction is less relevant and consequently, the diminution of K with temperature almost does not impact on limiting conversion.

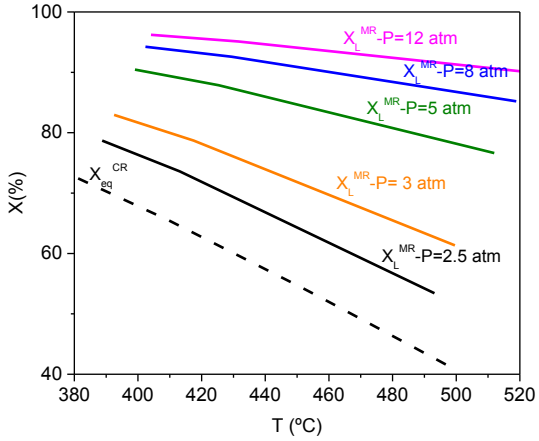

Fig. 4 – Limiting conversion curves (X_L^{MR} and X_{eq}^{CR}) vs. T, for different pressure values. Co-current configuration. $P_P = 1$ atm.

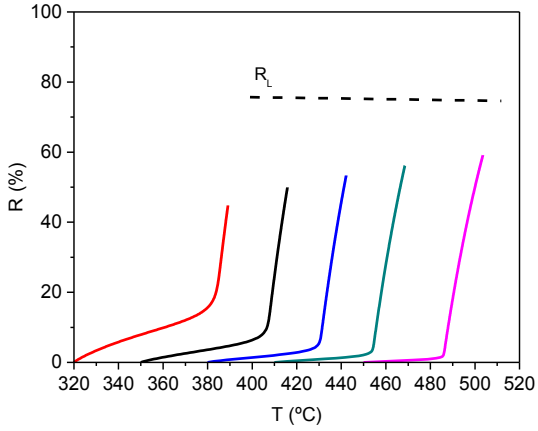

Fig. 6 – Recovery-Temperature Trajectories. P = 5 atm. Co-current configuration.

Similar results were obtained by Gallucci et al. [20]. However, it is important to highlight that in the present study no sweep gas was considered, i.e., the driving force is only given by pressure difference.

If the limiting conversion of a membrane reactor is estimated from Eq. (13), the limiting hydrogen flowrate at retentate side can be calculated by means of hydrogen stoichiometric balance and hydrogen flowrate at permeate sides can be calculated combining hydrogen stoichiometric balance at the retentate side and hydrogen partial pressures. Therefore, the limiting recovery (R_L) results:

$$R_L = \frac{\left(1 - \frac{F_{To}P_P}{\left(F_{H_2,o} + F_{CO,o}X_L^{MR}\right)P}\right)}{\left(1 - \frac{P_P}{P}\right)} \tag{14}$$

Figs. 5 and 6 show X_{CO}-T and R-T trajectories in the membrane reactor that correspond to the results presented in Fig. 2. The equilibrium conversion of the conventional reactor X_{eq}^{CR}, and limiting conversion of the membrane reactor X_L^{MR}, are also included in Fig. 5. Fig. 6 shows the limiting recovery (R_L).

In Fig. 5, it is possible to observe that X_{CO}-T trajectories present an almost linear behavior described by Eq. (15) and CO conversions of the membrane reactor are higher than the equilibrium conversion corresponding to the conventional reactor under the studied conditions. These differences are higher as T_o increases. Additionally, it is possible to observe that lower values of T_o lead to higher inlet-outlet temperature increments inside the membrane reactor (T(z) y T_P(z) are overlapped). This behavior is in accordance with:

$$\Delta T(z) = \Delta T_{ad} X_{CO}(z) \tag{15}$$

which defines that the temperature increment inside the membrane reactor operating without sweep gas is directly proportional to CO conversion levels achieved inside the reactor as previously demonstrated for high values of the product between the overall heat transfer coefficients (U) and the heat transfer area ($\pi n_t d_i$) [45].

The dependence of equilibrium conversion on temperature is more important in a conventional reactor than in a membrane reactor. If the reactor achieves its limiting condition (infinite reactor length), the limiting temperature could be estimated for a given inlet temperature combining Eqs. (13) and (15).

On the other hand, Fig. 6 shows that the limiting recovery (R_L) is almost independent from temperature at P = 5 atm, while the outlet hydrogen recovery increases with inlet temperature.

The behavior of a membrane reactor clearly improves with temperature due to higher hydrogen flowrates, associated with lower conversion and temperature rises inside the reactor. The differences between the outlet recovery values and the limiting recovery values (R_L) reveal that the recovery values could increase if the membrane area or the palladium thickness decreases.

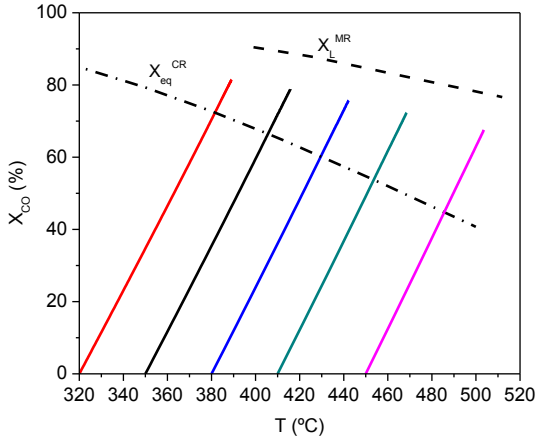

Fig. 5 – X_{CO}-T Trajectories. P = 5 atm.

Membrane reactor operating with steam as sweep gas

As previously mentioned (Section 1), the permeation driving force will increase if a sweep gas flowrate is fed in the permeate side operating under atmospheric pressure. However, the permeate stream, i.e., sweep gas and hydrogen, should be purified downstream the reactor with its associated costs. An interesting alternative for the WGS membrane

reactor is to employ a condensable sweep gas, e.g., steam in order to simplify its separation [49,50].

In this section, a different design from previously described is studied. For membrane reactor design 2 (D2) steam is employed as sweep gas. As the scale under study is larger than lab-scale reactors, thermal effects could be important and therefore, they are studied. Under this design, there are two new degrees of freedom, i.e., sweep gas feed temperature (T_{Po}) and flowrate (F_{SG}). Operating pressure at the retentate and permeate sides remains constant and equal to 1 atm.

Study of main operating variables

Fig. 7 shows CO conversion (a), retentate and permeate temperature (b) and recovery axial profiles for different inlet temperatures T_o, keeping the inlet sweep gas temperature (T_{Po}) and sweep gas flowrate (F_{SG}) constant. It is possible to observe that although the conversion profiles differ depending on the different values of T_o, the outlet conversions present similar values. However, the outlet conversion reaches a maximum value at $T_o = 350$ °C, that is in accordance with the behavior of a reversible reaction limited by equilibrium. On the other hand, hydrogen recovery (Fig. 7c) increases with T_o.

The temperature inside the reactor diminishes after reaching a maximum value (except from $T_o = 320$ °C) while permeate temperature always increases (dashed lines). It is important to note that the temperature profiles obtained when operating with sweep gas (D2) differ from temperature profiles corresponding to operation without sweep gas (D1) (Fig. 2b). The presence of maximum temperature values is associated with the cooling action of the sweep gas (steam) that allows the removal of heat generated by reaction. This means that the reactor operates under non-isothermal conditions while, under D1, the reactor operates adiabatically because there is no presence of a heat-removing stream.

As a consequence, although it is possible to reach similar conversion values to those obtained when operating without sweep gas (Fig. 2a), the thermal levels reached inside the reactor are lower. However, lower thermal levels inside the reactor have a negative impact on hydrogen permeation, i.e., maximum recovery values of 40% are obtained for an inlet temperature (T_o) equal to 450 °C, while recovery values of 60% are achieved when operating without sweep gas (Fig. 2c).

Estimation of limiting condition

In addition to the expression employed to estimate the limiting conversion of a pressurized membrane reactor, an algebraic expression was obtained in order to estimate the limiting conversion of a membrane reactor operating with sweep gas.

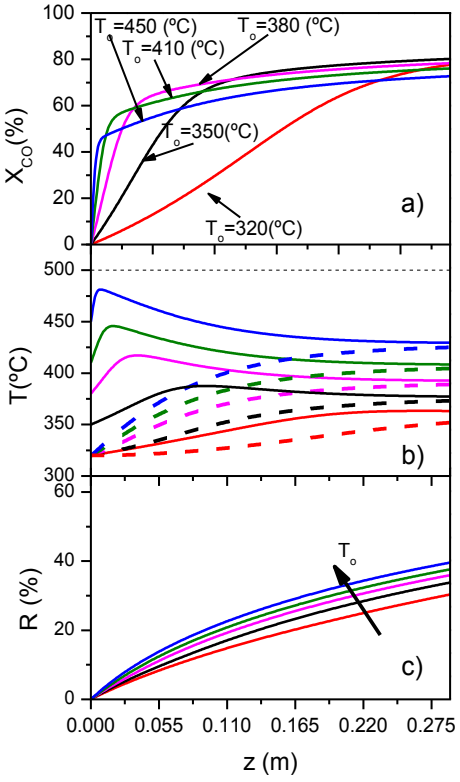

Fig. 7 – CO conversion (a), retentate and permeate temperature (b) and recovery (c) axial profiles at different T_o, corresponding to D2. $P = P_P = 1$ atm, $F_{SG} = 75\%\ F_{To}$, $T_{Po} = 320$ °C.

Combining the hydrogen stoichiometric balance and the equality of hydrogen partial pressures at both sides of the membrane ($p_{H_2} = p_{H_{2,P}}$), and considering that a sweep carrier gas is employed which generally means that the retentate side will not be pressurized, therefore, the assumption of $P = P_P = 1$ atm is valid and the permeated hydrogen flowrate can be estimated by means of Eq. (16):

$$F_{H_{2,P}} = \frac{F_{SG}\left(-F_{H_{2,o}} - F_{CO,o}X_L^{MR}\right)}{F_{H_{2,o}} + F_{CO,o}X_L^{MR} - F_{SG} - F_{To}} \tag{16}$$

When the hydrogen partial pressure equilibrium condition and Eq. (16) are replaced in the equilibrium constant expression (Eq. (12)), the limiting conversion of the membrane reactor can be estimated by means of Eq. (17):

$$f\left(X_L^{MR}\right) = exp^{(K)} - \frac{\left(F_{CO_2,o} + F_{CO,o}X_L^{MR}\right)\left(\frac{F_{SG}\left(-F_{H_{2,o}} - F_{CO,o}X_L^{MR}\right)}{F_{H_{2,o}} + F_{CO,o}X_L^{MR} - F_{SG} - F_{TO}}\right)\left(F_{TO} - \frac{F_{SG}\left(-F_{H_{2,o}} - F_{CO,o}X_L^{MR}\right)}{F_{H_{2,o}} + F_{CO,o}X_L^{MR} - F_{SG} - F_{TO}}\right)}{F_{CO,o}\left(1 - X_L^{MR}\right)\left(F_{H_2O,o} - F_{CO,o}X_L^{MR}\right)\left(\frac{F_{SG}\left(-F_{H_{2,o}} - F_{CO,o}X_L^{MR}\right)}{F_{H_{2,o}} + F_{CO,o}X_L^{MR} - F_{SG} - F_{TO}} + F_{SG}\right)} = 0 \tag{17}$$

The validity of Eq. (17) was verified simulating the membrane reactor long enough in order to achieve the limiting condition in the membrane reactor (MR). Fig. 8 shows X_L^{MR}-T_o equilibrium curves obtained for different sweep gas flowrates. It is possible to observe that the membrane reactor limiting conversion strongly depends on the sweep gas flowrate. Additionally, it is worth noticing that the dependence of X_L^{MR} on temperature is attenuated as the sweep gas flowrate increases. It is important to mention that, to our knowledge, no previous analysis of the influence of sweep gas flowrate on membrane reactor limiting conversion has been done.

Fig. 9 shows X_{CO}-T trajectories in the membrane reactor corresponding to the results shown in Fig. 7a and b. Equilibrium conversions corresponding to the conventional reactor X_{eq}^{CR} and limiting conversions corresponding to the membrane reactor (X_L^{MR}) are also presented in Fig. 9. As previously observed in Fig. 7a, an intermediate inlet temperature value of (≈350 °C) maximizes the conversion. This behavior is typical of an exothermic reaction limited by equilibrium. However, in a membrane reactor this maximum value of conversion could be achieved at higher temperatures [51,52].

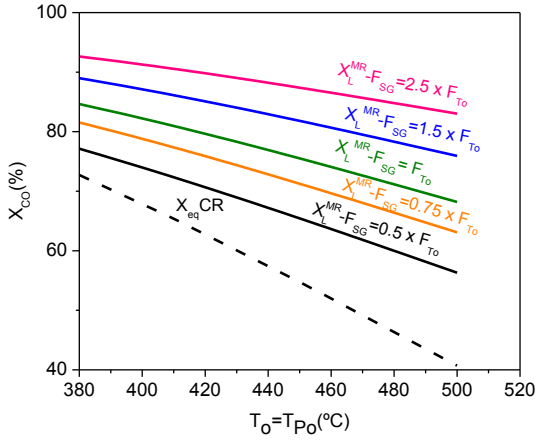

Fig. 8 – Limiting membrane reactor conversion, X_L^{MR}-T, for different F_{SG} values.

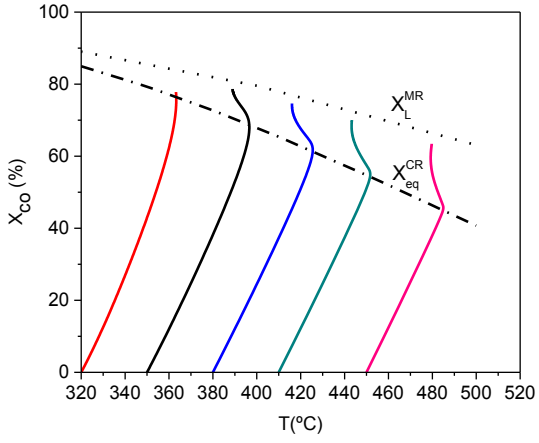

Fig. 9 – Trajectories X_{CO}-T. $P = P_P = 1$ atm, $F_{SG} = 75\%\ F_{To}$, $T_{Po} = 320$ °C.

When the hydrogen stoichiometric balance and the equation that estimates the hydrogen permeated flowrate (16) are replaced into Eq. (11) that defines hydrogen recovery, it is possible to obtain an expression in order to estimate the limiting hydrogen recovery value (R_L):

$$R_L = \frac{F_{SG}}{-F_{H_2,o} - F_{CO,o}X_L^{MR} + F_{SG} + F_{To}} \quad (18)$$

Fig. 10 shows R vs. T trajectories inside the reactor that result from combining Fig. 7b and c. The limiting recovery (R_L), estimated by means of (18), is also presented in Fig. 10. It is possible to observe that the recovery at the outlet of the membrane reactor improves as the inlet temperature increases and the limiting recovery value is almost independent from temperature.

Comparison between both models under study

In the present study, the most critical operating variables were analyzed for two different membrane reactor designs: D1 (without sweep gas) and D2 (steam as sweep gas). In both cases, temperature plays an important role, however, for D1 pressure (P) is another critical variable while for D2, is the sweep gas flowrate (F_{SG}).

The effect of pressure (P) on permeated hydrogen flowrate and CO conversion for two different values of T_o is presented in Fig. 11 for D1. While, Fig. 12 shows the effect of the sweep gas flowrate (F_{SG}) on permeated hydrogen flowrate and CO conversion for D2. Fig. 11 reaffirms the results previously discussed in Fig. 2. Hydrogen permeated flowrate is activated with temperature and conversion decreases with temperature. Summarizing, the optimal value of the feed temperature will depend on the expected hydrogen production and hydrogen recovery values taking into account also the temperature limits imposed by the materials of the membrane.

In Fig. 12, it is possible to observe that X_{CO} increases as sweep gas flowrate increases and then, remains insensitive to sweep gas flowrate changes. The permeated hydrogen flowrate increases, with temperature and sweep gas flowrate. However, as sweep gas flowrate increases, the difference between permeated hydrogen values at both temperatures is higher. Although in both cases (D1 vs. D2), the driving force for permeation increases when increasing pressure and sweep

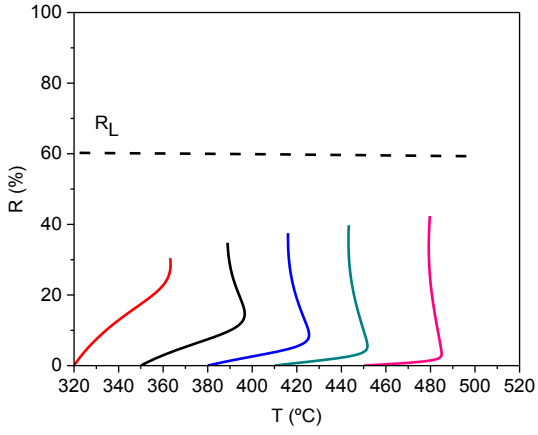

Fig. 10 – R-T Trajectories. $P = P_P = 1$ atm, $F_{SG} = 75\%F_{To}$, $T_{Po} = 320$ °C.

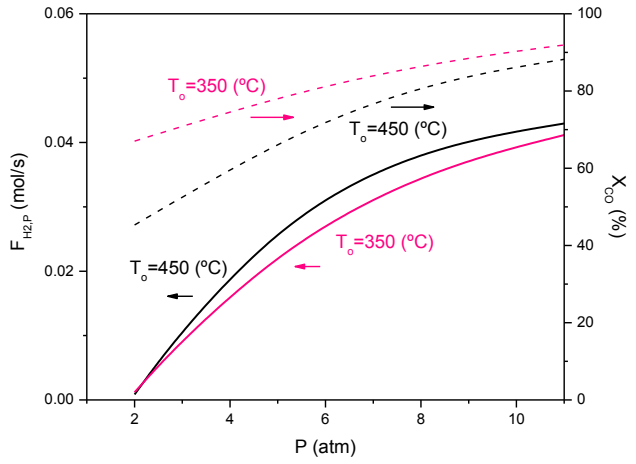

Fig. 11 – Hydrogen permeated flowrate and CO conversion vs. operating pressure for two values of T_o for D1.

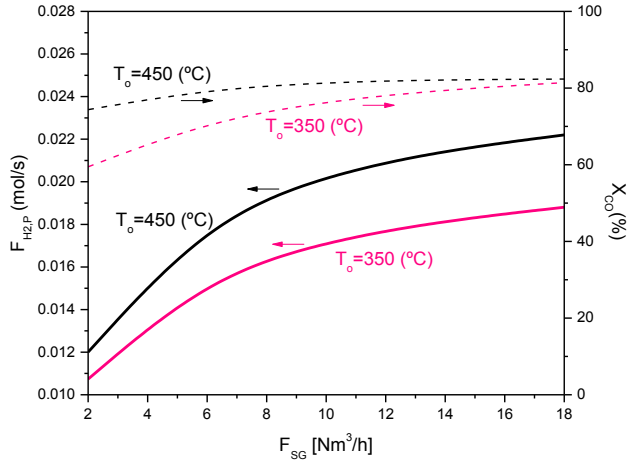

Fig. 12 – Hydrogen permeated flowrate and CO conversion vs. Sweep gas flowrate for two values of T_o and T_{Po} = 320 °C for D2.

gas flowrate respectively, for the D2 the sweep gas acts as a coolant diminishing the temperature inside the reactor and consequently, permeated hydrogen flowrate. It could be concluded that a pressure increment could have a better impact on membrane reactor performance because not only driving force increases but also the reactor achieves higher thermal levels that would contributes with permeation. The final decision on the operating conditions on the reactor should be based on an economic analysis, i.e., operating and capital costs.

Conclusions

In this work, the performance of a water gas shift membrane reactor operating with and without sweep gas was comparatively studied with special focus on thermal effects. The simulation results demonstrate that thermal effects play a key role in the operation of the water gas shift membrane reactor. It is possible to conclude that the membrane reactor should be operated at maximum allowable temperature values in order to maximize recovery or permeated hydrogen flowrate when operating with and without sweep gas. However, outlet CO conversion levels would be maximized at different temperature levels depending on the inlet composition and the operating conditions for both cases under comparison, i.e., with or without sweep gas. It is important to remark that these conclusions are subject to an inlet reactor flowrate containing hydrogen in its composition and consequently, will vary when feeding a reaction mixture of only CO y H_2O. The water gas shift membrane reactor process as intensification alternative for hydrogen generation-purification process largely behaves as a membrane separator because only 10% of total hydrogen is generated in it. Finally, novel-algebraic expressions that only depend on inlet conditions to estimate the limiting CO conversion and H_2 recovery are presented for a membrane reactor operating under concurrent configuration when operating without sweep gas. Additionally, the corresponding algebraic equations dependent only on inlet conditions are presented when operating with sweep gas constitute a useful complementary tool. If the hydrogen recovery (or CO conversion) experimentally measured (or estimated by means of a mathematical model) would be significantly lower than its limiting value, there were enough room to improve the hydrogen production through an increment in the membrane area or a diminution in the palladium thickness.

Acknowledgment

The authors want to thank the financial support from Consejo Nacional de Investigaciones Científicas y Técnicas (CONICET), Universidad Nacional del Sur (UNS) and Ministerio de Ciencia, Tecnología e Innovación Productiva (MINCyT).

Nomenclature

A_T	cross sectional area of catalyst bed, m^2
d_s	shell tube diameter, m
d_{te}	external tube diameter, m
d_{ti}	internal tube diameter, m
E_p	Activation energy of the hydrogen permeability, J/mol
F	molar flow, mol/s
J_{H_2}	permeation flow of hydrogen, mol/(s m^2)
L	tube length, m
N	number of components (reaction side)
p_i	partial pressure of component i, atm
r_{CO}	reaction rate, mol$_{CO}$/(kg$_{cat}$ s)
R	recovery
T	temperature, K
V_R	reactor volume, m^3
F_{To}	total feed flow rate, Nm^3/h
y	molar fraction
z	axial coordinate, m

Greek letters

δ	thickness of Pd film, μm

Subscripts

i	inlet
i	component i
T	total
o	at the axial coordinate z = 0
L	at the axial coordinate z = L
P	at permeation side
SG	sweep gas

Acronyms

WGS	water gas shift
MR	membrane reactor

REFERENCES

[1] Palo DR, Dagle RA, Holladay JD. Methanol steam reforming for hydrogen production. Chem Rev 2007;107(10):3992–4021.

[2] Francesconi JA, Mussati MC, Aguirre P. Analysis of design variables for water-gas-shift reactors by model-based optimization. J Power Sources 2007;173:467–77.

[3] Cornaglia L, Múnera J, Lombardo E. Recent advances in catalysts, palladium alloys and high temperature WGS membrane reactors: a review. Int J Hydrogen Energy 2015;40(8):3423–37.

[4] Criscuoli A, Basile A, Drioli E. An analysis of the performance of membrane reactors for the water–gas shift reaction using gas feed mixtures. Catal Today 2000;56:53–64.

[5] Uemiya S, Sato N, Ando H, Kikuchi E. The water gas shift reaction assisted by a palladium membrane reactor. Ind Eng Chem Res 1991;30:585–9.

[6] Basile A, Paturzo L, Galluci F. Co-current and counter-current modes for water gas shift membrane reactor. Catal Today 2003;82:275–81.

[7] Battersby S, Ladewig BP, Duke M, Rudolph V, Diniz da Costa JC. Membrane reactor modelling, validation and simulation for the WGS reaction using metal doped silica membranes. Asia-Pac J Chem Eng 2010;5(1):83–92.

[8] Boutikos P, Nikolakis V. A simulation study of the effect of operating and design parameters on the performance of a water gas shift membrane reactor. J Membr Sci 2010;350(1–2):378–86.

[9] Basile A, Curcio S, Bagnato G, Liguori S, Jokar SM, Iulianelli A. Water gas shift reaction in membrane reactors: theoretical investigation by artificial neural networks model and experimental validation. Int J Hydrogen Energy 2015;40:5897–906.

[10] Ghasemzadeha K, Zeynalia R, Basileb A. Theoretical study of hydrogen production using inorganic membrane reactors during WGS reaction. Int J Hydrogen Energy 2016;41(20):8696–705.

[11] Byron Smith RJ, Muruganandam L, Murthy Shekhar S. CFD analysis of water gas shift membrane reactor. Chem Eng Res Des 2011;89(11):2448–56.

[12] Coroneo M, Montante G, Catalano J, Paglianti A. Modelling the effect of operating conditions on hydrodynamics and mass transfer in a Pd–Ag membrane module for H_2 purification. J Membr Sci 2009;343:34–41.

[13] Ramasubramanian K, Song M, Ho WSW. Spiral-wound water-gas-shift membrane reactor for hydrogen purification. I.E.C Res 2013;52:8829–42.

[14] Chiappetta G, Clarizia G, Drioli E. Theoretical analysis of the effect of catalyst mass distribution and operation parameters on the performance of a Pd-based membrane reactor for water–gas shift reaction. Chem Eng J 2008;136:373–82.

[15] Chein R, Chen Y, Chung JN. Parametric study of membrane reactors for hydrogen production via high-temperature water gas shift reaction. Int J Hydrogen Energy 2013;38(5):2292–305.

[16] Sanz R, Calles JA, Alique D, Furones L, Ordóñez S, Marín P. Hydrogen production in a Pore-Plated Pd-membrane reactor: experimental analysis and model validation for the Water Gas Shift reaction. Int J Hydrogen Energy 2015;40(8):3472–84.

[17] Brunetti A, Caravella A, Barbieri G, Drioli E. Simulation of water gas shift reaction in a membrane reactor. J Membr Sci 2007;306:329–40.

[18] Koc R, Kazantzis N, Ma YH. Process safety aspects in water gas shift (WGS) membrane reactors used for pure hydrogen production. J Loss Prev Proc 2011;24:852–69.

[19] Marín P, Díez FV, Ordóñez S. Fixed bed membrane reactors for WGSR-based hydrogen production: optimisation of modelling approaches and reactor performance. Int J Hydrogen Energy 2012;37:4997–5010.

[20] Chein RY, Chen YC, Chung JN. Sweep gas flow effect on membrane reactor performance for hydrogen production from high-temperature water-gas shift reaction. J Membr Sci 2015;475:193–203.

[21] Hla SS, Morpeth L, Dolan M. Modelling and experimental studies of a water-gas shift catalytic membrane reactor. Chem Eng J 2015;276:289–302.

[22] Koukou MK, Papayannakos N, Markatos NC. On the importance of non-ideal flow effects in the operation of industrial-scale adiabatic membrane reactors. Chem Eng J 2001;83(2):95–105.

[23] Markatos NC, Vogiatzis E, Koukou MK, Papayannakos N. Membrane reactor modelling: a comparative study to evaluate the role of combined mass and heat dispersion in large-scale adiabatic membrane modules. Chem Eng Res Des 2005;83(A10):1171–8.

[24] Adrover ME, López E, Borio DO, Pedernera MN. Simulation of a membrane reactor for the WGS reaction: pressure and thermal effects. Chem Eng J 2009;154(1–3):196–202.

[25] Yua W, Ohmori T, Kataoka S, Yamamoto T, Endo A, Nakaiwa M, et al. A comparative simulation study of methane steam reforming in a porous ceramic membrane reactor using nitrogen and steam as sweep gases. Int J Hydrogen Energy 2008;33(2):685–92.

[26] Barbieri G, Marigliano G, Perri G, Drioli E. Conversion-temperature diagram for a palladium membrane reactor. Analysis of an endothermic reaction: methane steam reforming. Ind Eng Chem Res 2001;40:2017–26.

[27] Marigliano G, Barbieri G, Drioli E. Equilibrium conversion for a Pd-based membrane reactor. Dependence on the temperature and pressure. Chem Eng Process Process Intensif 2003;42(3):231–6.

[28] Hara S, Haraya K, Barbieri G, Drioli E. Estimating limit conversion for methane steam reforming in a palladium membrane reactor using countercurrent sweep gas. Asia-Pac J Chem Eng 2010;5:48–59.

[29] Gallucci F, De Falco M, Basile A. A simplified method for limit conversion calculation in membrane reactors. Asia-Pac J Chem Eng 2010;5:226–34.

[30] Adrover ME, López E, Borio DO, Pedernera MN. Theoretical study of a membrane reactor for the water gas shift reaction under nonisothermal conditions. AIChE J 2009;55(12):3206–13.

[31] Kikuchi E. Membrane reactor application to hydrogen production. Catal Today 2000;56:97–101.

[32] Mori N, Nakamura T, Noda K, Sakai O, Takahashi A, Ogawa N, et al. Reactor configuration and concentration

polarization in methane steam reforming by a membrane reactor with a highly hydrogen-permeable membrane. Ind Eng Chem Res 2007;46:1952–8.
[33] Lüdtke O, Behling R-D, Ohlrogge K. Concentration polarization in gas permeation. J Membr Sci 1998;146:145–57.
[34] Caravella A, Barbieri G, Drioli E. Modelling and simulation of hydrogen permeation through supported Pd-based membranes with a multicomponent approach. Chem Eng Sci 2008;63:2149–60.
[35] De Falco M. Membrane reactors modeling. In: De Falco M, Marrelli L, Iaquaniello G, editors. Membrane reactors for hydrogen production processes. London: Springer; 2011. p. 79–102.
[36] Adrover ME. Diseño y Simulación de reactors de membrane para la obtención y purificación de gas de síntesis [PhD thesis]. Universidad Nacional del Sur; 2009.
[37] Podolski WF, Kim YG. Modelling the water-gas shift reaction. Ind Eng Chem 1974;13(4):415–21.
[38] Reddy GK, Smirniotis PG. Water gas shift reaction research developments and applications. China: Elsevier B.V.; 2015.
[39] Barbieri G, Brunetti A, Granato T, Bernardo P, Drioli E. Engineering evaluations of a catalytic membrane reactor for the water gas shift reaction. Ind Eng Chem Res 2005;44:7676–83.
[40] Dixon AG. An improved equation for the overall heat transfer coefficient in packed beds. Chem Eng Process 1996;35:323–31.
[41] Dixon AG, Cresswell DL. Theoretical prediction of effective heat transfer parameters in packed beds. AIChE J 1979;25(4):663–76.
[42] De Falco M, Di Paola L, Marrelli L. Heat transfer and hydrogen permeability in modelling industrial membrane reactors for methane steam reforming. Int J Hydrogen Energy 2007;32:2902–13.
[43] Incropera FP, DeWitt DP. Fundamentos de Transferencia de calor y masa (4ta Edición). México: Prentice Hall Inc.; 1999.
[44] Hussain A, Seidel-Morgenstern A, Tsotsas E. Heat and mass transfer in tubular ceramic membranes for membrane reactors. Int J Heat Mass Transf 2006;49:2239–53.
[45] Adrover ME, Anzola A, Schbib S, Pedernera MN, Borio D. Effect of flow configuration on the behavior of a membrane reactor operating without sweep gas. Catal Today 2010;156(3–4):223–8.
[46] Newsome D. The water gas shift reaction. Catal Rev 1980;21(2):275–318.
[47] Amandusson H, Ekedahla L-G, Dabbetun H. Hydrogen permeation through surface modified Pd and Pd/Ag membranes. J Membr Sci 2001;193:21–36.
[48] McBride RB, McKinley DL. A new hydrogen recovery route. Chem Eng Prog 1965;61(3):81–5.
[49] Huang J. CO_2 (H_2S) membrane separations and WGS membrane reactor modeling for fuel cells [PhD thesis]. Ohio State University; 2007.
[50] Piemonte V, De Falco M, Favetta B, Basile A. Countercurrent membrane reactor for WGS process: membrane design. Int J Hydrogen Energy 2010;35:12609–17.
[51] Augustine AS, Ma YH, Kazantzis NK. High pressure palladium membrane reactor for the high temperature water gas shift reaction. Int J Hydrogen Energy 2011;36:5350–60.
[52] Barbieri G, Brunetti A, Tricoli G, Drioli E. An innovative configuration of a Pd-based membrane reactor for the production of pure hydrogen. Experimental analysis of water gas shift. J Power Sources 2008;182:160–7.